Journal of Colloid and Interface Science 352 (2010) 81–86

Contents lists available at ScienceDirect

Journal of Colloid and Interface Science

www.elsevier.com/locate/jcis

Hierarchical synthesis of silver nanoparticles and wires by copolymer templates and visible light

Yen-Chi Hsu [a], Yu-Min Chen [a], Wei-Li Lin [a], Yi-Fen Lan [a], Ying-Nan Chan [a], Jiang-Jen Lin [a,b,*]

[a] Institute of Polymer Science and Engineering, National Taiwan University, No. 1, Sec. 4, Roosevelt Road, Taipei 10617, Taiwan
[b] Department of Materials Science and Engineering, National Chung Hsing University, No. 250, Kou Kuang Road, Taichung 402, Taiwan

ARTICLE INFO

Article history:
Received 30 June 2010
Accepted 7 August 2010
Available online 19 August 2010

Keywords:
Self-assembly
Silver cubes
Silver wires
Photo-reduction

ABSTRACT

Self-assembled silver wires in micro-meter scale were obtained from aqueous silver nitrate solution in the presence of a comb-like copolymer as the sole organic component. The requisite copolymer was easily prepared by the grafting poly(oxyethylene)-monoamine (POE-amine) onto poly(styrene-*co*-maleic anhydride) (SMA). Upon storage at ambient temperature with exposure to daylight, the aqueous $AgNO_3$/SMA–POE solution gradually underwent a color changed from transparent pale-yellow to dark-violet over a period of hours, and after several months a solid precipitate was deposited. The formation process was monitored by ultraviolet–visible spectrometer, particle size analysis, scanning electron microscope, and transmission electron microscope. Silver wires were hierarchically formed by progressive transformation from the initial appearance of silver nanoparticles (*ca.* 10 nm in diameter), followed by the intermediate rectangles (0.6–1.0 μm in width and 0.4 μm in length) in solution and ultimately the precipitates in micro-scale of silver wires at 1.6–6.4 μm in diameter and 100–370 μm in length. The progressive formation of the precipitated silver wires was accelerated by the exposure of visible light as a photo-reducing energy source. The micron-scale wires have a silver content over 97.4 wt.% and a sheet resistance of 5.5×10^1 Ω/square.

1. Introduction

Recent developments of using bottom-up synthesis for the fabrication of nano- and micro-meter metal materials has found versatile material applications in electronic [1], optical [2] and biomedical areas [3]. In general, the nanometer-sized materials can be classified into three categories according to their geometric shapes: spherical particles, lengthy tubes, and thin platelets. One of the most intriguing self-assembly mechanisms is the progressive formation of unit interconnections, such as secondary structures of fibrous arrays from spherical particles. In nature, self-organizing mechanisms are ubiquitous in living matter, including the formation of grape-vine morphology in the growth of microorganisms and of fern-like arrays of fungi colonies and in the plant kingdom. In the realm of man-made materials, syntheses of nanoparticles [4], quantum dots [5] and one-dimensional nanowires [6] have been extensively reported for their potential applications in optical [7], electrical [8–12] and magnetic devices [13].

Among synthetic nanomaterials, silver nanoparticles (AgNPs) are well-known for their unique antimicrobial [14] and electronic conducting properties [15]. In general, the synthesis involves the reduction of silver ions (Ag^+) in the presence of organic stabilizers [16] and reducing agents [17]. Furthermore, silver nanostructures of various shapes [18], including spherical, triangular and fibrous morphologies have been reported by using polymer templates, including block copolymers [19–21], DNA [22,23], poly(acrylic acid) (PAA) [24], poly(vinyl pyrrolidone) (PVP) [25–27], poly(vinyl alcohol) (PVA) [28] and poly(styrene-*alt*-maleic anhydride) (SMA) [29]. Organic surfactants such as cetyltrimethylammonium bromide (CTAB) [30] may be present to form rod-shaped micelles which consequently direct the formation of the silver morphology. Sodium borohydride [31,32], formaldehyde [33], hydrazine [34,35], ethylene glycol [27] and poly(ethylene glycol) (PEG) [36] are commonly used as reducing agents. Physical methods such as photo-reduction [37–39], ultraviolet light [40], microwaves [41] and the involvement of organic polymers such as PVA [40] and PEG [36] have been reported in the literatures.

In the present study, we first used a comb-like copolymer as a template to control the hierarchical formation of rectangle-united silver fibrous wires in daylight. The synthesis [42], amphiphilicity [43] and pH-thermoresponse [44] of grafting poly(oxyethylene) [POE] segmented monoamine onto SMA have been extensively studied in our laboratory. The copolymer possesses multiple amidoacid

* Corresponding author at: Institute of Polymer Science and Engineering, National Taiwan University, No. 1, Sec. 4, Roosevelt Road, Taipei 10617, Taiwan. Fax: +886 2 3362 5237.

E-mail addresses: d94549006@ntu.edu.tw (Y.-C. Hsu), d94549005@ntu.edu.tw (Y.-M. Chen), r97549017@ntu.edu.tw (W.-L. Lin), d95549006@ntu.edu.tw (Y.-F. Lan), jan.in.nan@gmail.com (Y.-N. Chan), jianglin@ntu.edu.tw (J.-J. Lin).

0021-9797/$ - see front matter © 2010 Elsevier Inc. All rights reserved.
doi:10.1016/j.jcis.2010.08.024

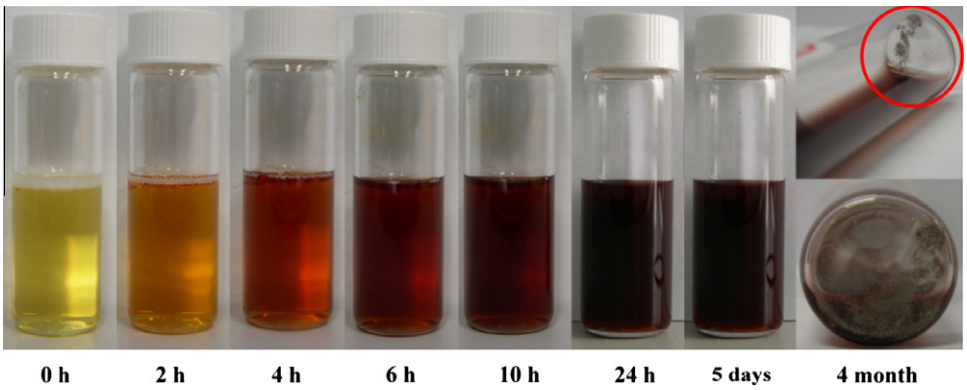

Fig. 1. Color changes of the solution from light yellow to dark-violet and appearance of solid precipitates during the storage of $AgNO_3$/SMA–POE aqueous solution. (For interpretation of the references to colour in this figure legend, the reader is referred to the web version of this article.)

polar functionalities for association with Ag^+. Under visible light enhancement, Ag^+ was gradually reduced to AgNPs which subsequently self-assembled into micro-sized wires in the presence of the polymer template.

2. Experimental

2.1. Materials

The copolymer, poly(styrene-*co*-maleic anhydride) (SMA) with styrene/maleic anhydride (ST/MA) molar ratios of 2:1 in the backbones, was purchased from Aldrich Chemical Co., and named as SMA2000. The average molecular weight was estimated to be 6000 M_w by gel permeation chromatography (GPC) using polystyrene as the standard. The poly(oxyethylene–oxypropylene)-monoamine (POE-amine) with the designated trade names of Jeffamine® M2070 (abbreviated M2070) was obtained from Huntsman Chemical Co. The amine, hydrophilic and water-soluble, has a backbone of oxyethylene/oxypropylene blocks at 32/10 unit molar ratio with an average molecular weight of 2000 M_w. Silver nitrate ($AgNO_3$, 99.8%) was purchased from SHOWA Chemical Co.

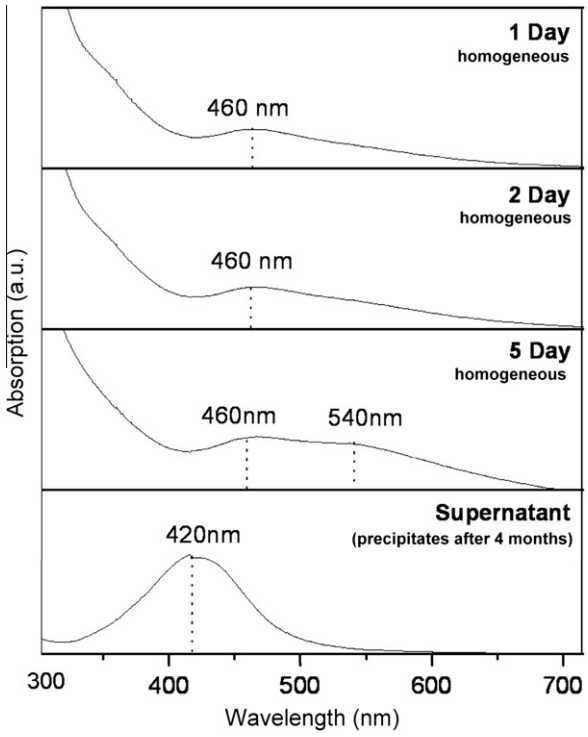

Fig. 2. UV–vis analyses of $AgNO_3$/SMA–POE solution in water during 1–5 days and the supernatant after the formation of precipitates.

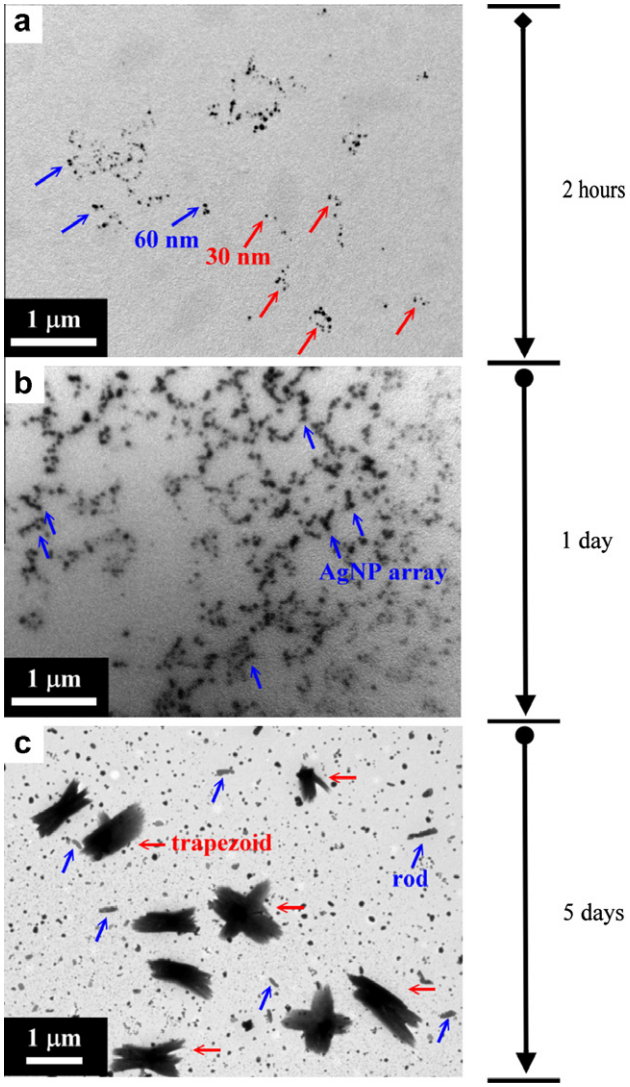

Fig. 3. TEM images of the $AgNO_3$/SMA–POE solution over a long period of time (a) initial solution (b and c) formation of spherical and trapezoidal arrays.

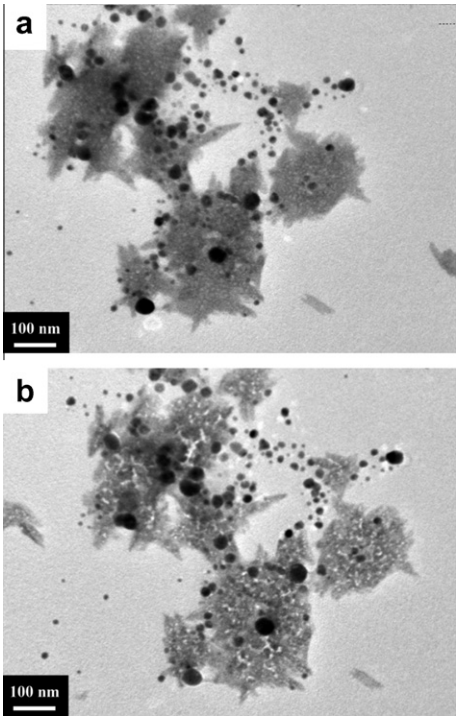

Fig. 4. TEM images of spherical Ag^0 and trapezoidal Ag^0/SMA–POE complex (incubated for 5 days) under the irradiation of TEM electron beam; (a) initial (b) after 30 min irradiation.

2.2. Instruments

The surface analyses were performed by field emission scanning electron microscope (FE-SEM) with JOEL JSM-6700F and operated at the 15 kV. Transmission electronic microscope (TEM) was performed with a Zeiss EM 902A and operated at 80 kV. X-ray powder diffraction (XRD) (Schimadzu SD-D1 using a Cu target at 35 kV, 30 mA) was used to measure the lattice of silver atoms in the crystal form. XRD were operating at a scanning rate of 1°/s in 2θ ranging from 2° to 120°. Ultraviolet–visible (UV–vis) spectrometer was recorded on Shimadzu UV-1240. The absorption of fourier-transform infrared spectroscopy (FT-IR) was measured by using a Perkin–Elmer Spectrum 100 FTIR Spectrometer. The surface element analysis was performed on an energy dispersive X-ray spectroscopy (EDS, Hitachi SR845). A Zeta Plus zetameter (Brookhaven Instrument Corp., NJ) was used for characterizing the average particle size in diameter of the SMA–POE copolymer and AgNPs.

2.3. Preparation of the SMA2000-POE copolymer

The preparation of POE-amine graft SMA2000 copolymers (SMA–POE) was reported previously in our laboratory [42–44]. Typical procedures for preparing POE-amine grafted SMA2000 at 1:1 MA/NH_2 molar ratio are described below. The SMA2000 (10.0 g, 32.7 mmol of MA) was added drop-wise to the M2070 (65.4 g, 32.7 mmol of NH_2) in tetrahydrofuran (THF, 50 mL) and stirred at 25 °C for 2–3 h. During the process, samples were taken periodically and monitored by using a FT-IR. The absorption peaks

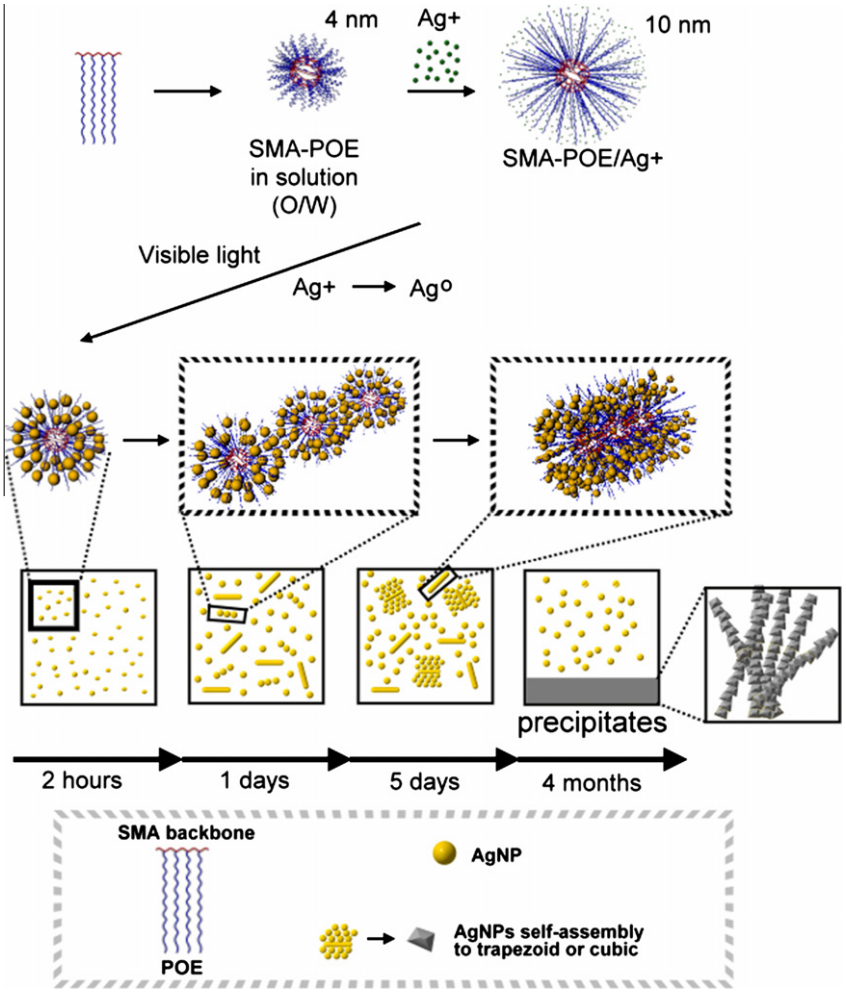

Fig. 5. Conceptual diagram of hierarchical formation from polymer template, silver reduction into nanoparticles, and self-assembled silver fibrous wires.

at 1734 cm^{-1} and 1690 cm^{-1} for the carboxylic acid and amide functionalities, respectively, appeared at the expense of anhydride absorption at 1780 cm^{-1} (s) and 1850 cm^{-1} (w). Another characteristic absorption at 1100 cm^{-1} of oxyalkylene was observed.

2.4. Preparation of silver self-assemblies

Silver nitrate (0.20 g) in water (0.50 g) and added into solution of SMA–POE copolymer (0.50 g in 0.5 g water). The mixture solution was placed in a test tube and vigorously mixed by shaking for 3 min. The homogenized solution was light-colored, but gradually changed into pale-yellow and dark-violet under visible light during several days in storage. After standing for a long period of 4 months, a solid precipitate appeared at the bottom of the flask. The precipitates were collected at ambient temperature, washed thoroughly with de-ionized water, and dried under vacuum. The sample morphology was analyzed by XRD, FE-SEM, EDS and TGA. The morphological variation of the collected silver wires after heating to 100, 200, 250 and 900 °C for each 1 h under nitrogen atmosphere was then observed by FE-SEM. The melting phenomenon on the wire surfaces and the connection between the wires are observed. The sheet resistance was measured by QUATEK QT50 using four-point probe of the Hp 4338B Milliohmeter according to ASTM Method D257-93. The sheet resistance is expressed in Ohms/square or Ω/square, in which the size of the square is immaterial.

3. Results and discussion

The synthesis of AgNPs generally involves the use of reducing agents [31–36] and organic stabilizers [19–29]. In this study, $AgNO_3$ was reduced in the presence of POE-functionalized SMA copolymers under exposure to visible light. It was found that, with the assistance of SMA–POE copolymer, an aqueous solution of $AgNO_3$ was slowly reduced and changed color from pale-yellow to dark-violet over a period of 24 h, as indicated by the pictures in Fig. 1. After standing for 5 days, the solution maintained a dark color, but some solid precipitate appeared. The color changes implied the occurrence of Ag^+ reduction of Ag^+ to AgNPs [45]. The whole process was apparently induced by visible light. In a control experiment, when the sample was stored in a vial wrapped with aluminum foil to exclude light, the solution did not change color or form a solid precipitate over the same period of storage time.

The process of AgNPs formation could be monitored by UV–vis absorption (Fig. 2), with the characteristic absorption at 460 nm signaling the presence of AgNPs on the first and second days. Another absorption at 540 nm appeared after 5 days, indicating a secondary species of AgNPs. After 4 months of induction time, precipitation occurred and the suspension displayed another absorption signal at 420 nm, which indicated the presence of smaller AgNPs. The absorptions at 460 and 540 nm disappeared due to the precipitation of secondary AgNPs at the bottom of solution. In

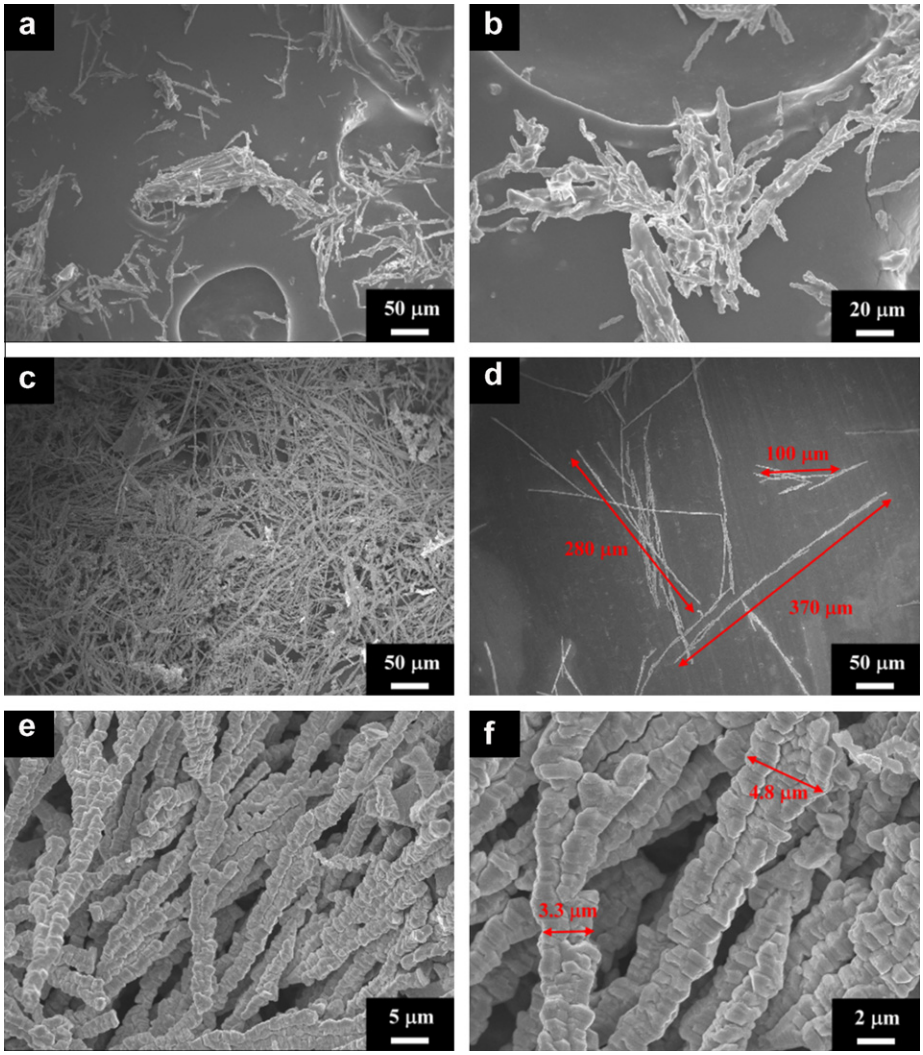

Fig. 6. FE-SEM images of the precipitates before (a and b) and after water washing (c–f).

this reduction profile, Ag^+ was first bound at the carboxylic amido-acid sites [24] and then at the poly(oxyethylene) [i.e. $(CH_2CH_2O)_x$] segment [46] of the SMA2000-M2070 copolymer through a chelating mechanism and then reduced to AgNPs.

When examined by TEM, as shown in Fig. 3, the appearance of longitudinal silver rods were observed after the sample has been stored for 5 days. Initially, after 2 h of storage, the TEM morphology of the sample revealed spherical shapes of AgNPs with particle sizes from 30 to 60 nm (Fig. 3a). After 2 days of storage, more particles and array of AgNPs were observed (Fig. 3b). After 5 days of storage (Fig. 3c), secondary AgNPs with a trapezoid shape and lengthy rods were formed. The spherical vs. trapezoid is roughly estimated to be 62:19 in number. Since the size of the latter is much larger, the area ratio representing to the mass ratio is also estimated to be 13:85 in the 5-day sample. Apparently, the coexistence of spherical particles, progressively larger cubes and longitudinal rods revealed the sequence of the self-assembly of the AgNPs. Initially, the amphiphilic SMA–POE copolymer formed the polymeric micelles, which was evidenced by the presence of particles of average diameter 4 nm when the solution was analyzed by means of a Zeta Plus zetameter (Fig. S1). After addition of aqueous $AgNO_3$ to the copolymer solution, the SMA–POE micelles served as templates for chelating the Ag^+ through the POE pendant groups and functional amidoacids [45]. The particle size of the SMA–POE/Ag^+ micelles increased to 10 nm in diameter, which was maintained over 3 days, indicating the adsorption of Ag^+ onto the polymer templates (Fig. S1). Furthermore, the copolymer micelle/Ag^+ complex may serve as a template for orientating silver growth after the addition of $AgNO_3$ and the ability of the copolymer to lower the surface tension in water was measured (Fig. S2). Both the copolymer and its Ag^+ complex exhibited a similar ability to lower the surface tension in water, indicating that the copolymer-Ag^+ complex maintained their micelle structures.

For the kinetic transformation of the silver arrays, only spherical AgNPs were observed after 2 h by TEM (Fig. 3a) and characterized by ultraviolet–visible spectrometer at *ca.* 460 nm. After standing for 1 day, more AgNPs arrays had been formed (Fig. 3b), which subsequently self-assembled into rod-like and trapezoidal AgNPs after 5 days (Fig. 3c). Both the rod-like and trapezoidal AgNPs may be regarded as templates for Ag^+ absorption or Ag^0 formation, and further self-aggregated and precipitated into irregular shapes of micro arrays after standing for 4 months. In order to characterize the silver trapezoids, the trapezoidal AgNPs were exposed to an electron beam for 30 min (Fig. 4). Under the high-energy exposure, the AgNPs maintained their morphology, indicating that the trapezoidal particles contained Ag^0 instead of Ag^+. The trapezoids were also examined by the selected-area electron diffraction (SAED), which indicated that the structure was polycrystalline in nature (Fig. S3). In a hierarchical manner, the self-assembly involves the initial formation of polymeric templates, which lead to the reduction of Ag^+ to spherical Ag^0. Further aggregation created the series of nano-rods and trapezoids, and finally the Ag wire precipitated from the solution. The proposed formation mechanism is conceptually described in Fig. 5.

The precipitate was analyzed by FE-SEM, which revealed the directional, ordered wire bundles (Fig. 6a and b). The collected precipitate was further washed several times with de-ionized water to remove the absorbed SMA–POE organic copolymer. The purified precipitates revealed wire-like fibers with high uniformity and had dimension of 1.6–6.4 μm in diameter and 100–370 μm in length (Fig. 6c and d). The magnified surface morphology of the fibers was seen to be ladder-shaped with the units of stacked trapezoid cubes (Fig. 6e and f). Individual cubes had an average size of 3.3–4.8 μm in rectangle shape. It appeared that the cubes were stacked in both vertical and horizontal directions to form wires.

The purified precipitate consisting of wire-like fibers was further characterized by XRD and the XRD pattern showed the lattice constant of the silver fiber was calculated to be 4.0677 Å, which is closest to the literature data (a = 4.0862 Å JCPDS File 04-0783) that indicate a crystal of *fcc* phase (Fig. S4). As showed in Fig. S5, elemental analyses of the fibers by used EDS revealed the Ag^0 (*ca.* 97.4 wt.% or 80.9 mol%) as the major constituent, along with some carbon content (2.56 wt.% or 19.1 mol%). The presence of carbon suggests polymer incorporation between the cube interfaces that result from the cube stacking. For practical applications, the melting and electrical resistance properties of the wire-like fibers were

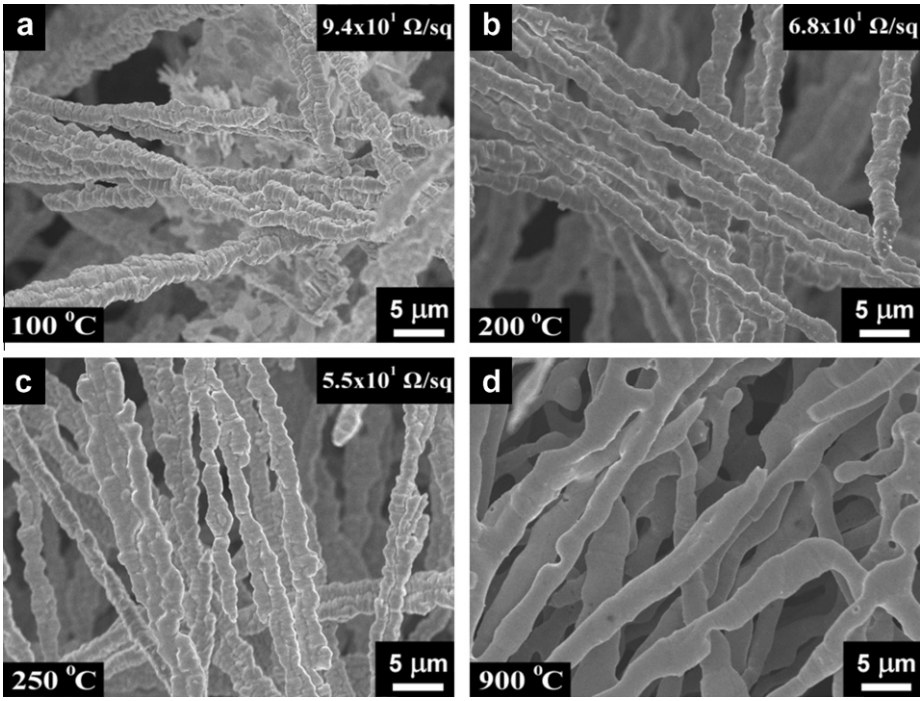

Fig. 7. Surface morphological changes of silver wires heated at 100, 200, 250 and 900 °C for each 1 h.

studied. In Fig. 7, the results further demonstrate the morphological changes into a progressively smoother silver wire surface with ongoing thermal treatment at 100, 200, 250 and 900 °C. The micrographs indicate that the silver wires melted at 200 °C and that the melted surface was welded along a single silver wire, possibly adhering into a cross-linked network structure. The images demonstrate an initial melting at 200 °C and more thoroughly melting at 900 °C. The low sheet resistance of 9.4×10^1 Ω/square was obtained due to the high content of silver (97.4 wt.% from EDS). After heating from 25 °C to 100, 200 and 250 °C, the sheet resistance of Ag wire showed a slightly decreased from 9.4×10^1 Ω/square to $6.8–5.5 \times 10^1$ Ω/square, respectively.

4. Conclusion

With a copolymer template and radiation by visible light, silver nitrate was reduced to silver nanoparticles, which continued to transform into self-aggregated longitudinal rods and eventually lengthy fibrous wires. The comb-branched SMA–POE copolymers used was essential for directing this hierarchical self-assembly. In the process, visible light is required for the initial silver ion reduction. The observation of transformation of AgNPs into lengthy silver wires in micro-meter scale reveals the diversity of copolymer templates for the self-assembly as well as a facile method for the potential bottom-up synthesis of micro-conductors.

Acknowledgments

We acknowledge financial supports from the Ministry of Economic Affairs and National Science Council (NSC) of Taiwan.

Appendix A. Supplementary material

Supplementary data associated with this article can be found, in the online version, at doi:10.1016/j.jcis.2010.08.024.

References

[1] M. Antonietti, C. Goltner, Angew. Chem., Int. Ed. 36 (1997) 910.
[2] B.J. Wiley, Y. Chen, J. McLellan, Y. Xiong, Z.Y. Li, D. Ginger, Y. Xia, Nano Lett. 7 (2007) 1032.
[3] X. Huang, I.H. El-Sayed, W. Qian, M.A. El-Sayed, J. Am. Chem. Soc. 128 (2006) 2115.
[4] J. Schmitt, G. Decher, W.J. Dressick, S.L. Brandow, R.E. Geer, R. Shashidhar, J.M. Calvert, Adv. Mater. 9 (1997) 61.
[5] I.L. Medintz, H.T. Uyeda, E.R. Goldman, H. Mattoussi, Nat. Mater. 4 (2005) 435.
[6] J. Hu, T.W. Odom, C.M. Lieber, Acc. Chem. Res. 32 (1999) 435.
[7] M.S. Gudiksen, L.J. Lauhon, J. Wang, D.C. Smith, C.M. Lieber, Nature 415 (2002) 617.
[8] S. Förster, M. Antonietti, Adv. Mater. 10 (1998) 195.
[9] M. Moffitt, A. Eisenberg, Chem. Mater. 7 (1995) 1178.
[10] F. Favier, E.C. Walter, M.P. Zach, T. Benter, R.M. Penner, Science 293 (2001) 2227.
[11] Y. Cui, Q. Wei, H. Park, C.M. Lieber, Science 293 (2001) 1289.
[12] M. Zayats, R. Baron, I. Popov, I. Willner, Nano Lett. 5 (2005) 21.
[13] F.Y. Cheng, C.H. Su, Y.S. Yang, C.S. Yeh, C.Y. Tsai, C.L. Wu, M.T. Wu, D.B. Shieh, Biomaterials 26 (2005) 729.
[14] I. Sondi, B.J. Salopek-Sondi, J. Colloid Interface Sci. 275 (2004) 177.
[15] H.H. Lee, K.S. Chou, K.C. Huang, Nanotechnology 16 (2005) 2436.
[16] A. Henglein, M. Giersig, J. Phys. Chem. B 103 (1999) 9533.
[17] G.N. Glavee, K.J. Klabunde, C.M. Sorensen, G.C. Hadjipanayis, Langmuir 9 (1993) 162.
[18] Y. Sun, Y. Xia, Science 298 (2002) 2176.
[19] D. Zhang, L. Qi, J. Ma, H. Cheng, Chem. Mater. 13 (2001) 2753.
[20] B.H. Sohn, R.E. Cohen, J. Appl. Polym. Sci. 65 (1997) 723.
[21] J.J.L.M. Cornelissen, R. van Heerbeek, P.C.J. Kamer, J.N.H. Reek, N.A.J.M. Sommerdijk, R.J.M. Nolte, Adv. Mater. 14 (2002) 489.
[22] E. Braun, Y. Eichen, U. Sivan, G. Ben-Yoseph, Nature 391 (1998) 775.
[23] A.A. Zinchenko, K. Yoshikawa, D. Baigl, Adv. Mater. 17 (2005) 2820.
[24] J. Bai, Y. Qin, C. Jiang, L. Qi, Chem. Mater. 19 (2007) 3367.
[25] Y. Sun, B. Gates, B. Mayers, Y. Xia, Nano Lett. 2 (2002) 165.
[26] Y. Sun, B. Mayers, T. Herricks, Y. Xia, Nano Lett. 3 (2003) 955.
[27] Y. Sun, Y. Yin, B.T. Mayers, T. Herricks, Y. Xia, Chem. Mater. 14 (2002) 4736.
[28] L.B. Luo, S.H. Yu, H.S. Qian, T. Zhou, J. Am. Chem. Soc. 127 (2005) 2822.
[29] T.D. Lazzara, G.R. Bourret, R.B. Lennox, G.M. Theo, Chem. Mater. 21 (2009) 2020.
[30] C.J. Murphy, N.R. Jana, Adv. Mater. 14 (2002) 80.
[31] Z. Zhang, R.C. Patel, R. Kothari, C.P. Johnson, S.E. Friberg, P.A. Aikens, J. Phys. Chem. B 104 (2000) 1176.
[32] P. Setua, A. Chakraborty, D. Seth, M.U. Bhatta, P.V. Satyam, N. Sarkar, J. Phys. Chem. C 111 (2007) 3901.
[33] T.I. Taylor, W.H. Cone, J. Am. Chem. Soc. 55 (1933) 3512.
[34] Y. Li, Y. Wu, B.S. Ong, J. Am. Chem. Soc. 127 (2005) 3266.
[35] T.H. James, J. Am. Chem. Soc. 62 (1940) 1654.
[36] M.N. Nadagouda, R.S. Varma, Cryst. Growth Des. 8 (2008) 291.
[37] A. Callegari, D. Tonti, M. Chergui, Nano Lett. 3 (2003) 1565.
[38] M. Maillard, P. Huang, L. Brus, Nano Lett. 3 (2003) 1611.
[39] S. Kapoor, Langmuir 14 (1998) 1021.
[40] Y. Zhou, S.H. Yu, C.Y. Wang, X.G. Li, Y.R. Zhu, Z.Y. Chen, Adv. Mater. 11 (1999) 850.
[41] L. Gou, M. Chipara, J.M. Zaleski, Chem. Mater. 19 (2007) 1755.
[42] K.L. Wei, J.Y. Wu, Y.M. Chen, Y.C. Hsu, J.J. Lin, J. Appl. Polym. Sci. 103 (2007) 716.
[43] J.J. Lin, Y.C. Hsu, K.L. Wei, Macromolecules 40 (2007) 1579.
[44] J.J. Lin, Y.C. Hsu, J. Colloid Interface Sci. 336 (2009) 82.
[45] Y. Yang, J. Shi, T. Tanaka, M. Nogami, Langmuir 23 (2007) 12042.
[46] D.H. Chen, Y.W. Huang, J. Colloid Interface Sci. 255 (2002) 299.